REGULAR ARTICLE

blood advances

MLL leukemia induction by t(9;11) chromosomal translocation in human hematopoietic stem cells using genome editing

Corina Schneidawind,[1,2,*] Johan Jeong,[1,*] Dominik Schneidawind,[2] In-Suk Kim,[1,3] Jesús Duque-Afonso,[1,4] Stephen Hon Kit Wong,[1] Masayuki Iwasaki,[1] Erin H. Breese,[5] James L. Zehnder,[1,6] Matthew Porteus,[7] and Michael L. Cleary[1]

[1]Department of Pathology, Stanford University, Stanford, CA; [2]Department of Hematology and Oncology, University Hospital Tuebingen, Tuebingen, Germany; [3]Department of Laboratory Medicine, Pusan National University Yangsan Hospital, Yangsan, Korea; [4]Department of Hematology and Oncology, University Medical Center Freiburg, Freiburg, Germany; [5]Cancer and Blood Diseases Institute, Division of Oncology, Cincinnati Children's Hospital Medical Center, Department of Pediatrics, University of Cincinnati, Cincinnati, OH; and [6]Division of Hematology, Department of Medicine, and [7]Division of Stem Cell Transplantation and Regenerative Medicine, Department of Pediatrics, Stanford University, Stanford, CA

Key Points

- Genome editing induces t(9;11) chromosomal translocations and transforms primary CD34$^+$ human cord blood cells leading to acute leukemia.
- CD9 is upregulated in primary t(9;11) cells and is a useful marker for enrichment of genome-edited *MLL*-rearranged cells in vitro.

Genome editing provides a potential approach to model de novo leukemogenesis in primary human hematopoietic stem and progenitor cells (HSPCs) through induction of chromosomal translocations by targeted DNA double-strand breaks. However, very low efficiency of translocations and lack of markers for translocated cells serve as barriers to their characterization and model development. Here, we used transcription activator-like effector nucleases to generate t(9;11) chromosomal translocations encoding *MLL-AF9* and reciprocal *AF9-MLL* fusion products in CD34$^+$ human cord blood cells. Selected cytokine combinations enabled monoclonal outgrowth and immortalization of initially rare translocated cells, which were distinguished by elevated *MLL* target gene expression, high surface CD9 expression, and increased colony-forming ability. Subsequent transplantation into immune-compromised mice induced myeloid leukemias within 48 weeks, whose pathologic and molecular features extensively overlap with de novo patient *MLL*-rearranged leukemias. No secondary pathogenic mutations were revealed by targeted exome sequencing and whole genome RNA-sequencing analyses, suggesting the genetic sufficiency of t(9;11) translocation for leukemia development from human HSPCs. Thus, genome editing enables modeling of human acute *MLL*-rearranged leukemia in vivo, reflecting the genetic simplicity of this disease, and provides an experimental platform for biological and disease-modeling applications.

Introduction

Leukemias constitute a heterogeneous group of diseases defined by their diverse molecular abnormalities, which dictate disease pathogenesis, treatment response, and clinical prognosis.[1] The *MLL/KMT2A* proto-oncogene is a frequent target for chromosomal translocations in a subset of acute leukemia that is generally associated with a poor prognosis.[2] The roles of MLL fusion proteins have been investigated in various model systems, each of which has specific technical advantages as well as limitations with uncertain implications for human *MLL* leukemia pathogenesis.[3-8] Recently, we used custom nucleases for genome editing to activate *MLL* oncogenes in primary human hematopoietic stem and progenitor cells (HSPCs) that generated leukemia after transplantation in mice.[9] Although this knock-in approach recapitulated many features of the clinical disease presented in patients, it did not reconstitute all genetic aspects of the disease context (eg, lacking the reciprocal product of the

Submitted 28 October 2017; accepted 1 March 2018. DOI 10.1182/bloodadvances.2017013748.

*C.S. and J.J. contributed equally to this study.

The full-text version of this article contains a data supplement.

translocation).[9] However, induction of reciprocal *MLL-AF4* and *MLL-AF9* translocations in vitro resulted in translocated cell frequencies that were extremely low, and the cells died out during long-term culture and failed to induce leukemia in mice.[10] These findings are supported by other studies showing that the generation of translocations using human primary cells is not robust, with detectable translocation frequencies between 1×10^{-3} and 1×10^{-5} independent of the type of nucleases employed for genome editing.[11-14] Despite the increasing feasibility of using novel genome editing tools to generate alterations in primary human HSPCs mimicking the nature of patient disease, it remains difficult to achieve sufficient numbers due to both low efficiency as well as the lack of marker proteins that allow for selective recognition and analysis of the translocated cells.

In this report, we employed non–virally expressed transcription activator-like effector nucleases (TALENs) to specifically engineer reciprocal chromosomal translocations of the *MLL* and *AF9* genes in primary human HSPCs that induced myeloid leukemias in transplanted mice and shared pathologic and molecular features with patient *MLL*-rearranged (*MLL*r) acute myeloid leukemia (AML). Our results demonstrate that optimized culture conditions and surface markers expressed preferentially on the translocated cells can overcome the existing limitations in genome editing techniques to induce chromosomal translocations in primary human HSPCs and develop reliable in vivo models of human *MLL*r leukemia.

Methods

TALENs

TALENs targeting the *MLL*[9] and *AF9*[10] genes have been described previously.

Cell culture and nucleofection

$CD34^+$ HSPCs were isolated from fresh human umbilical cord blood (huCB) obtained from the maternity ward of Stanford Hospital (under an institutional review board–approved research protocol) and maintained as previously described,[9] with the following changes: granulocyte colony-stimulating factor (G-CSF) (50 ng/mL, PeproTech) and UM729 (0.75 μM, STEMCELL Technologies) were added into the culture media. A total of 300 000 $CD34^+$ cells were nucleofected in one reaction, and the viability (30% to 50%) and nucleofection efficiency (40% to 70% GFP positive) were measured by flow cytometry 2 days after nucleofection. Nucleofected cells were incubated at 37°C, 5% CO_2 in serum-free media (StemSpan II) plus cytokines, 20 μM Z-Vad-FMK (Enzo Life Sciences), and Rho-associated kinase pathway inhibitor/thiazovivin (STEMCELL Technologies), and 20% filtered fetal bovine serum was added 48 hours later. Viable cell counts were assessed 2 to 3 times per week, and cultures were split into fresh media to maintain a cell density of 7.5×10^5 cells/mL.

Humanized *MLL-AF9* leukemia model

Monoclonal *MLL-AF9* translocated cells were transplanted into immune-compromised NOD.*Cg-PrkdcscidIL2rgtm1Wjl*/SzJ (NSG) mice as previously described.[9] Primary recipient female NSG mice were sublethally irradiated (200 cGy), and xenotransplants were performed either by IV injection with 2×10^6 or intrafemoral injection with 1×10^6 *MLL-AF9*–rearranged cells. Human cell engraftment in the bone marrow was determined by the detection of human CD45 by flow cytometry. All experiments on mice were performed with the approval of and in accordance with the Stanford University Administrative Panel on Laboratory Animal Care.

PCR for translocation detection and sequencing

For each polymerase chain reaction (PCR), 150 ng genomic DNA was used with the translocation-specific primers listed in supplemental Table 1. The following PCR parameters were used: denature at 95°C for 5 min (denature at 95°C for 30 s and anneal at 60°C for 45 s, with extension at 72°C for 1 min) for 35 cycles, and final extension at 72°C for 5 min. PCR products were visualized on a 1% agarose gel with ethidium bromide. PCR products were extracted from the gel (QIAGEN), cloned into the pCRII-Blunt-TOPO vector (Invitrogen), and transformed into competent cells. Plasmid DNA of the transformed competent cells was subjected to Sanger sequencing using the M13 forward and M13 reverse primers.

RT-PCR and qPCR

RNA was isolated using the RNeasy Mini Kit (QIAGEN) and used to generate complementary DNA using the SuperScript III First-Strand Synthesis System (Invitrogen). PCR was subsequently performed for *MLL-AF9* and *AF9-MLL* fusion transcripts with the reverse transcription polymerase chain reaction (RT-PCR) primers listed in supplemental Table 1. PCR products were visualized, gel extracted, and subjected to Sanger sequencing. Quantitative PCR (qPCR) was performed for detection of target genes *MEIS1* (HS00180020_m1), *HOXA6* (HS00430615_m1), *HOXA9* (HS00266821_m1), and *HOXA10* (HS00365956_m1) by qPCR TaqMan Gene Expression Assays (Life Technologies).[15] qPCR was performed in triplicate followed by melting curve analysis in the Bio-Rad CFX384 C1000 Real-Time System. Cq values of undetectable transcripts were artificially set to the maximum amplification cycle numbers. Results were normalized to the housekeeping gene *ACTB* and then compared with the value of Mono Mac-6.

Flow cytometry and FACS

Analyses were performed using an LSR II flow cytometer (BD Biosciences). Fluorescence-activated cell sorting (FACS) was performed by using a FACS Aria (BD Biosciences) and FACS DIVA software (BD Biosciences). Data were analyzed using FlowJo volume 10 (Tree Star). For analysis, the following fluorochrome-conjugated monoclonal antibodies were used: CD34-allophycocyanin (clone 4H11, eBioscience), CD38-phycoerythrin /Cy7 (clone HIT2, BioLegend), CD33-PerCP/Cy5.5 (clone WM53, BioLegend), CD14-Alexa Fluor 700 (clone HCD14, BioLegend), CD64-allophycocyanin/Cy7 (clone 10.1, BioLegend), CD117-brilliant violet 421 (clone104D2, BioLegend), CD15-PerCP/Cy5.5 (clone W6D3, BioLegend), and CD9-phycoerythrin (clone eBioSN4/SN4 C3-3A2, eBioscience)

Results

TALEN-mediated genome editing of primary human HSPCs induces t(9;11) chromosomal translocations and *MLL* fusion gene expression

To induce t(9;11) translocations in HSPCs, $CD34^+$ cells isolated from huCB were nucleofected with 4 plasmids expressing 2 sets of TALENs targeting *MLL* or *AF9*, respectively (supplemental Figure 1). Plasmids encoding *GFP* or TALENs targeting only *MLL*

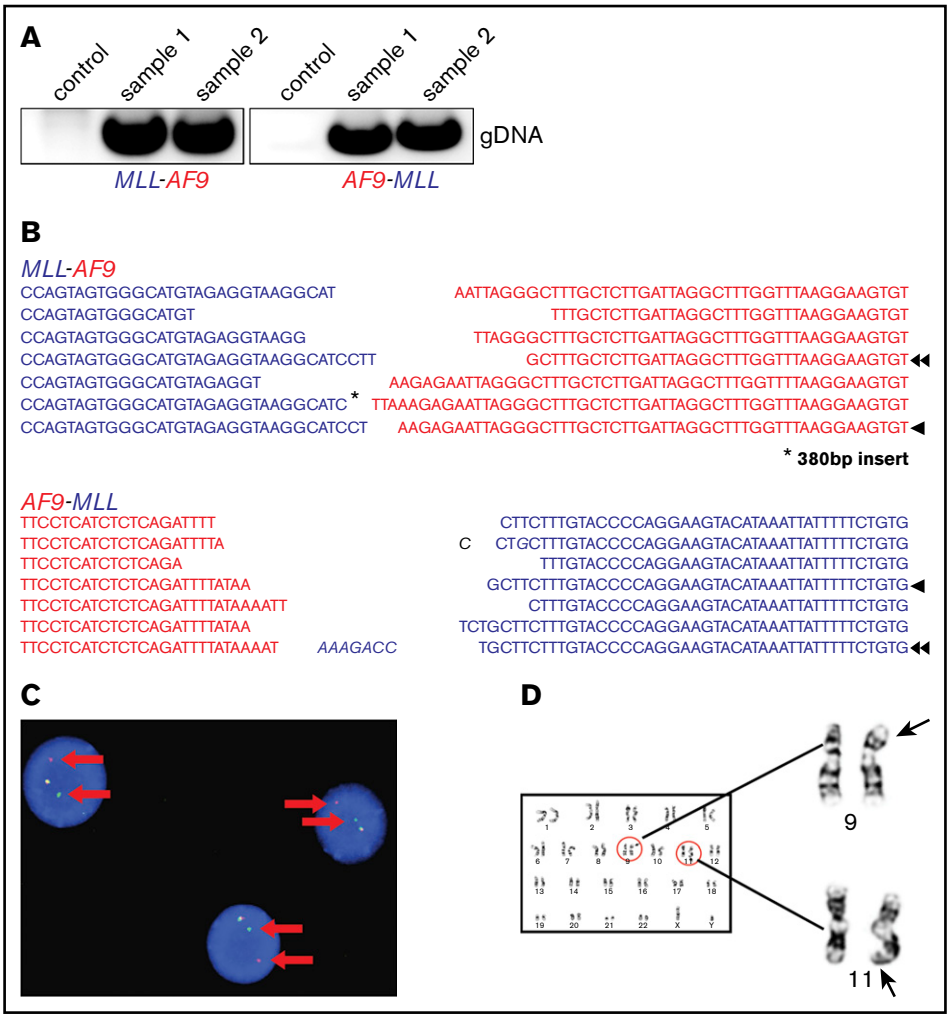

Figure 1. Molecular and cytogenetic features of *MLL-AF9*–rearranged cells induced by genome editing. (A) Representative PCR to detect *MLL-AF9* (left) and *AF9-MLL* (right) translocation breakpoints in gene-edited cells at day 27 of culture (samples 1 and 2). (B) Data shown are a composite alignment of PCR products from multiple experiments (days 7-14 of culture) showing a variety of distinct translocations. Arrowheads indicate the sequence of long-term–survived clones. (C) FISH analysis using an *MLL* break-apart probe was performed on genome-edited cells maintained in culture for over 50 days. A representative image is shown. Arrows indicate the split signals of the break-apart probe indicating *MLL* translocation. (D) Representative metaphase chromosomes from karyotype analysis of genome-edited cells shows a balanced t(9;11) chromosomal translocation.

were used as controls. The TALENs were designed to cleave intron 11 of the *MLL* gene and intron 5 of the *AF9* gene, respectively, corresponding to the genomic regions of frequent chromosomal translocation breakpoints in patients with *MLL-AF9* leukemias.[3,9,10] After nucleofection, the unselected cell population was maintained in vitro in liquid culture (~0.75 × 10^6/mL) supplemented with cytokines (stem cell factor [SCF], thrombopoietin, FLT3L, interleukin-6 [IL-6], IL-3, and G-CSF) and aryl hydrocarbon receptor antagonists (SR1 and UM729) optimized for growth of normal human HSPCs.[16,17]

MLL-AF9 and *AF9-MLL* fusion junctions were detected by PCR in 4 out of 8 TALEN-treated samples, 2 of which showed long-term outgrowth (Figure 1A) during extended in vitro culture. Sanger sequencing demonstrated that the PCR products in early cultures (days 7-14) constituted a heterogeneous mixture of several fusion sequences (Figure 1B). To confirm the chromosomal rearrangements and quantify the percentage of cells with translocations, fluorescence in situ hybridization (FISH) and karyotype analyses were performed. On day 54 in liquid culture, an *MLL* break-apart probe detected *MLL* translocations in 96% and 78% of the genome-edited cells, respectively, in 2 independent cultures (Figure 1C), which increased to 100% by day 76. G-banding analyses demonstrated the presence of both derivative chromosomes 9 and 11 resulting from reciprocal t(9;11) translocation (Figure 1D).

RT-PCR analysis revealed the expression of *MLL-AF9* fusion transcripts as in the *MLL-AF9* human leukemia cell line Mono Mac 6 vs non-*MLL*r control cells (Figure 2A). Two alternatively transcribed fusion transcripts were detected as previously reported in *MLL-AF9* cell lines and patient samples.[18,19] Western blot analysis demonstrated the presence of *MLL-AF9* fusion proteins at comparable levels to the *MLL-AF9* cell line (Figure 2B). Similarly, the genome-edited *MLL-AF9* cells demonstrated increased expression levels of common *MLL* target genes (*MEIS1*, *HOXA6*, *HOXA9*, and *HOXA10*) compared with control cells (Figure 2C). These results indicate that TALEN-mediated genome editing targeting *MLL* and *AF9* creates t(9;11) chromosomal translocations, which result in *MLL-AF9* gene fusions, which in turn induce *MLL* target gene expression at levels comparable to human leukemia cell lines harboring similar chromosomal translocations.

Genome-edited *MLL-AF9*-rearranged cells display distinct cytokine requirements for proliferation and maturation arrest

To assess their cytokine requirements, proliferation of the translocated cells was measured after three days culture in the presence of aryl hydrocarbon receptor inhibitors SR-1 and UM729 with single cytokines. Under these conditions, only IL-3 or SCF alone

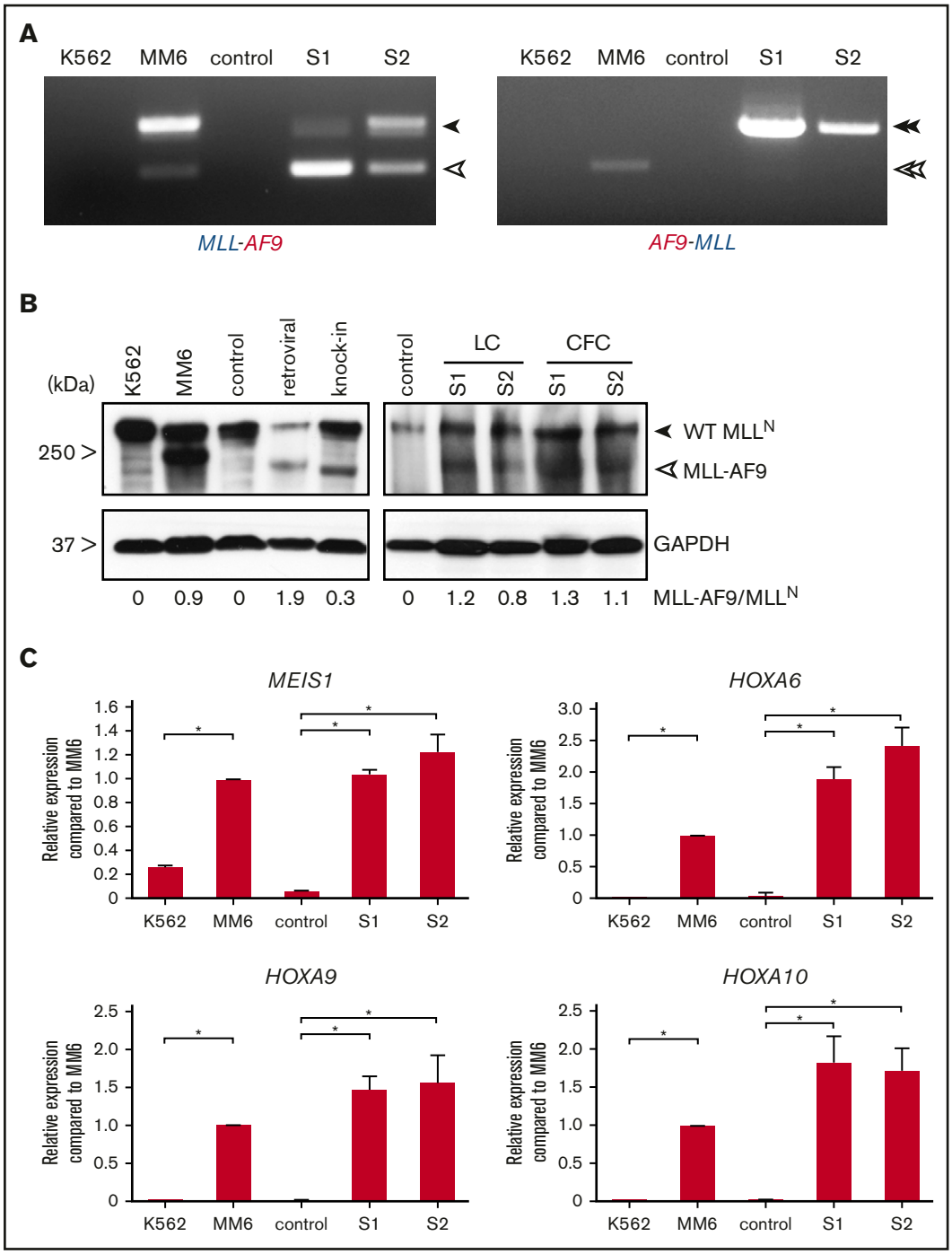

Figure 2. Transcriptional features of genome-edited *MLL-AF9* translocated cells. (A) RT-PCR was performed on complementary DNA of genome-edited *MLL*r cells from 2 independent cultures to detect fusion transcripts. Closed arrowheads indicate *MLL-AF9* and *AF9-MLL* fusion transcripts. Open arrowheads indicate the alternatively processed fusion transcripts, which lack *MLL* exon 11 and *MLL* exon 12 from *MLL-AF9* and *AF9-MLL*, respectively. (B) Representative western blot analysis of *MLL* proteins in controls (nucleofected with *GFP* alone) and *MLL-AF9*–rearranged cells cultured either in liquid or semisolid medium. Retroviral and knock-in indicate transformed human cord blood cells by retroviral *MLL-AF9* or *MLL-AF9* knock-in. CFC, colony-formed cells; GAPDH, loading control; LC, liquid culture. Numbers below indicate relative *MLL-AF9* band intensities compared with WT MLL^N. (C) Representative qPCR analyses show expression levels of *MLL* target genes compared with control (nucleofected with *GFP*) at day 65 of culture and human leukemia cell lines. $*P < .02$. Error bars indicate standard deviation of triplicate analyses. MM6, Mono Mac 6; S1, sample 1; S2, sample 2; WT, wild-type.

supported robust proliferation (Figure 3A). To further assess the necessary combination of cytokines, cells were cultured for an additional 7 and 17 days (total of 27 days) in cytokine milieus containing IL-3 or SCF and additionally one of the remaining cytokines of the standard culture conditions (Figure 3B). Whereas IL-3 alone was sufficient to sustain proliferation, it was further

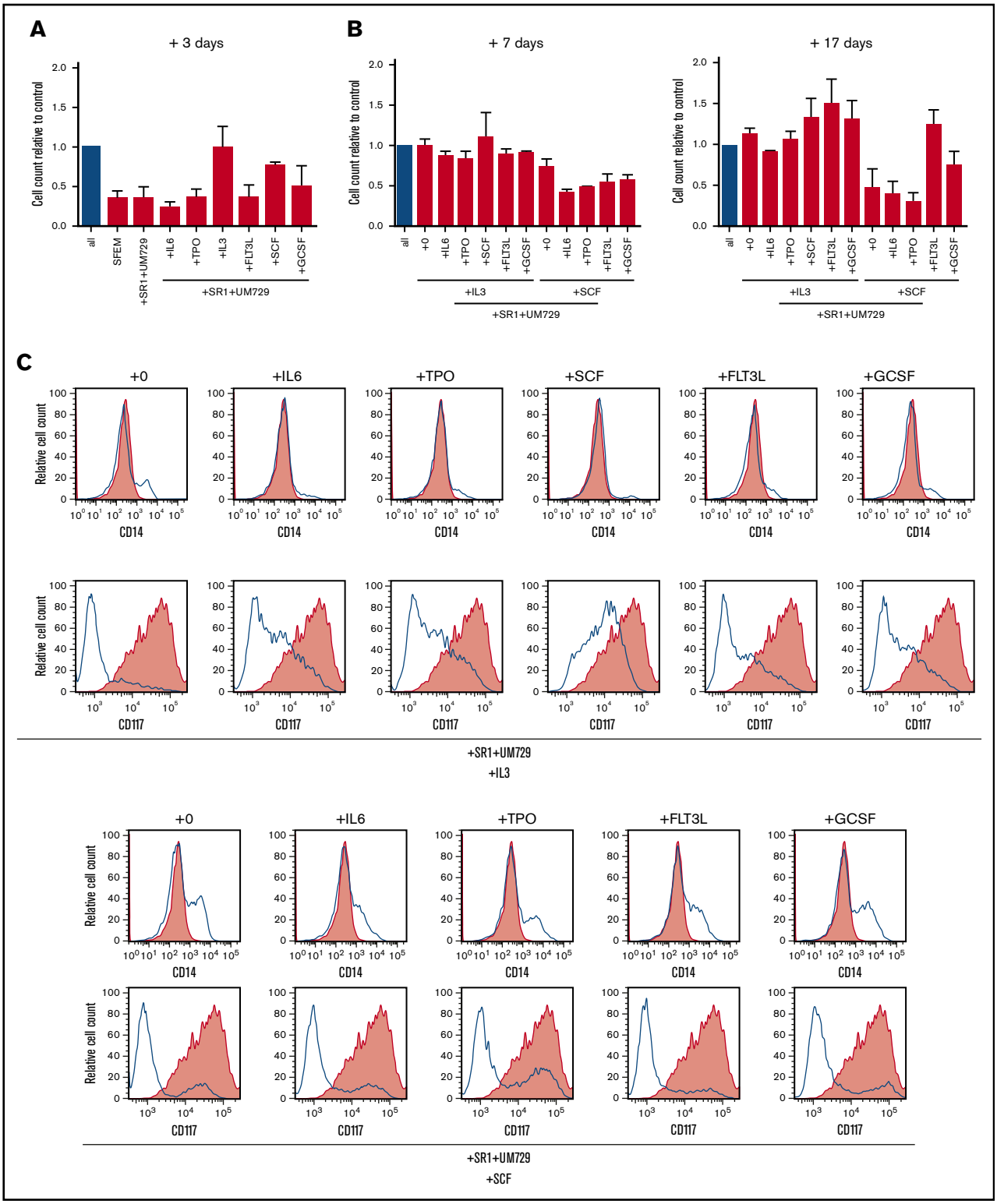

Figure 3. *MLL-AF9* translocated cells display specific cytokine dependence profiles. (A) *MLL-AF9*–rearranged cells cultured in the presence of SR-1 and UM729 plus the indicated single cytokines were quantified by trypan blue dye exclusion after 3 days and compared with control (all cytokines, blue bar). (B) Cells cultured with IL-3 or SCF were additionally cultured for 7 and 17 days in the presence of SR-1, UM729, the respective cytokines IL-3 or SCF, and the indicated single cytokine to evaluate their sensitivity compared with the control (all cytokines, blue bar). Error bars indicate SEM for 2 analyses. (C) Flow cytometry profiles show representative phenotypes of cells cultured in the indicated cytokine milieus after 27 days (blue lines) vs cells culture in the complete cytokine cocktail (red shading). TPO, thrombopoietin.

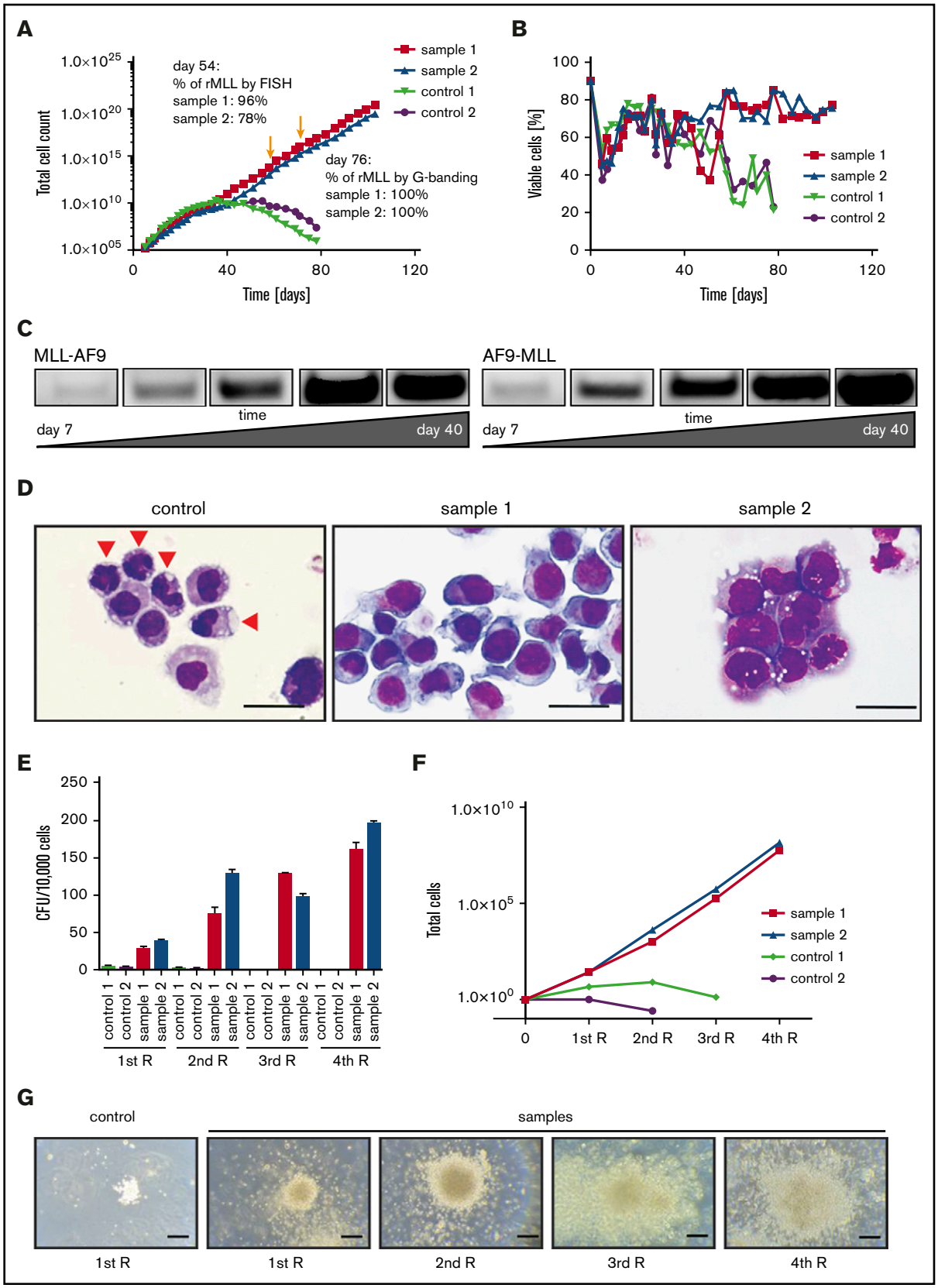

Figure 4. Genome-edited primary CD34$^+$ cells display survival advantage and clonal expansion in vitro. (A) Representative growth curves chart the differences in proliferative capacity of genome-edited CD34$^+$ cells compared with controls (*GFP* or *MLL* TALENs alone). Arrows indicate time point of FISH analyses and karyotyping.

increased by the addition of SCF, FLT3L, or G-CSF. Conversely, SCF alone was not sufficient to support proliferation in long-term culture but was partially rescued by the addition of G-CSF and completely rescued by the addition of FLT3L, indicating important roles for both cytokines. Interestingly, cells cultured with SCF alone showed not only a decrease of cell proliferation but also an increase in cell differentiation after 27 days of culture, indicated by the loss of immature marker CD117 and gain of maturation marker CD14 (Figure 3C). Whereas IL-3 was the major driving factor for proliferation, the inclusion of other cytokines present in our standard culture conditions was necessary to prevent maturation. These results demonstrate that *MLL-AF9* translocated cells remain cytokine dependent for in vitro proliferation and maturation arrest.

TALEN-induced chromosomal translocations in primary CD34$^+$ cells confer enhanced long-term proliferation and survival in vitro

In long-term culture, the numbers of gene-edited *MLL-AF9* cells progressively increased while control cell proliferation peaked at around day 40 and decreased afterward (Figure 4A). Similarly, viability of control cells declined after day 40, whereas *MLL-AF9* cells maintained their viability (Figure 4B). PCR analysis of DNA from the cultures of gene-edited cells showed an extremely low level of *MLL-AF9* and *AF9-MLL* fusion junctions in early cultures (day 7) with progressive increase as culture time proceeded (Figure 4C). Sanger sequencing of PCR bands at day 40 revealed that long-term cultures typically contained one distinct translocation product for the *MLL-AF9* fusion and the reciprocal *AF9-MLL* fusion, respectively (Figure 1B, arrowheads), indicating that a single clone of cells with the *MLL-AF9* translocation outgrew in each of the cultures.

Consistent with this, *MLL-AF9*–rearranged cells displayed immature morphologies in contrast to the differentiated control cells (Figure 4D). Following transfer at day 60 from liquid to semisolid medium supplemented with the same cytokines as the liquid culture, *MLL-AF9* translocated cells formed predominantly compact colonies that increased in size and numbers as well as cell counts after each round of plating, whereas control cells were unable to form compact colonies and failed to replate (Figure 4E-G). These studies demonstrate that generation of *MLL-AF9* chromosomal translocations by genome editing stimulates the long-term growth and survival of primary human HSPCs.

MLL-AF9 translocated cells display immature phenotypes and preferentially express CD9

The clonal cells bearing t(9;11) chromosomal translocations displayed immature myelomonocytic phenotypes with expression of CD34 and CD117 with virtually no expression of the mature marker CD14, whereas control cells lacked immature markers and displayed high expression of CD14, indicating that in long-term liquid culture conditions, genome-edited CD34$^+$ cells had markedly impaired terminal myeloid differentiation (Figure 5A).

Similar to the previous reports that CD9 is preferentially expressed on *MLLr* acute lymphoblastic leukemia (ALL) cells, but not normal cells from the same patient,[20] most of the *MLL-AF9* translocated cells expressed CD9 irrespective of CD34 status, in contrast to control cells, which lacked CD9 expression (Figure 5A). CD9 expression progressively increased over time in culture comparable to PCR band intensity of *MLL-AF9* and reciprocal *AF9-MLL* fusions (compare Figure 4C and Figure 5B), suggesting a positive correlation between CD9 expression and translocation.

To assess the relationship between t(9;11) chromosomal rearrangement and CD9 expression, CD9-positive and CD9-negative cells on day 36 of culture were sorted by FACS and subjected to FISH analysis. Unsorted cells showed a FISH signal in 12% of cells, whereas ~60% of CD9-positive sorted cells were FISH positive compared with 1% of CD9-negative sorted cells (Figure 5C). Colony-forming assays also showed a substantial enrichment of clonogenic cells in the CD9-positive versus negative *MLL*r populations (supplemental Figure S2A), indicating a positive correlation between self-renewal and CD9 expression of *MLL-AF9* translocated cells.

CD9 is highly expressed on primary *MLL*r patient AML cells (Figure 5D) and was increased in *MLL*r AMLs compared with non-*MLL*r AMLs in previously published datasets (supplemental Figure 2C).[21,22] In contrast, only a small minority of mononuclear cells from bone marrow and cord blood of healthy donors expressed CD9, which was predominantly restricted to the CD34$^-$ population (supplemental Figure 2B). Thus, acute induction of *MLL-AF9* chromosomal translocation antagonizes differentiation of CD34$^+$ cells in prolonged in vitro culture and presents CD9 as a surface marker for their identification and enrichment

MLL-AF9 translocated cells created by genome editing induce AML without evidence of secondary genetic mutations

Immune-compromised NSG mice were transplanted with genome-edited cells harvested from cultures containing 100% t(9;11) cells by FISH analysis (Figures 4A and 6A). The cells were transplanted IV (2×10^6) or intrafemorally (1×10^6) directly from liquid media.[9] Cells engrafted into recipient mice (tail vein 72.7%, n = 11; femur 37.5%, n = 8; Table 1) and developed leukemia with a mean latency of ~48 weeks (~37-60 weeks, n = 10; Figure 6B; Tables 1 and 2).

Transplanted mice with disease symptoms were euthanized for analysis. Leukemic mice shared similar disease profiles characterized by blasts in peripheral blood (Figure 6C), hypercellular bone marrow with human blast cells, myelomonocytic differentiation and occasional megakaryocytic hyperplasia (Figure 6D,F), splenomegaly (Figure 6E), and infiltration of peripheral tissues (Figure 6F).

Figure 4. (continued) (B) Graph shows cell viability in liquid culture monitored over time by flow cytometry and further confirmed by trypan blue dye exclusion. (C) PCR was performed for *MLL-AF9* and reciprocal *AF9-MLL* breakpoints on genomic DNA over progressive time of culture. (D) Representative morphologies are shown for control and translocated cells on day 76 by May-Grünwald-Giemsa staining. Arrowheads indicate differentiating cells. Scale bar, 20 μm. (E) Colony-forming assays were performed on day 60 of liquid culture. Bars represent the mean number of colony-forming units (CFUs) per 10^4 seeded cells. (F) Plot indicates cell numbers after each replating. Experiments were performed in triplicate, and data from 2 independent experiments are shown. (G) Images show representative morphologies of colonies after each replating (R). Scale bar, 200 μm.

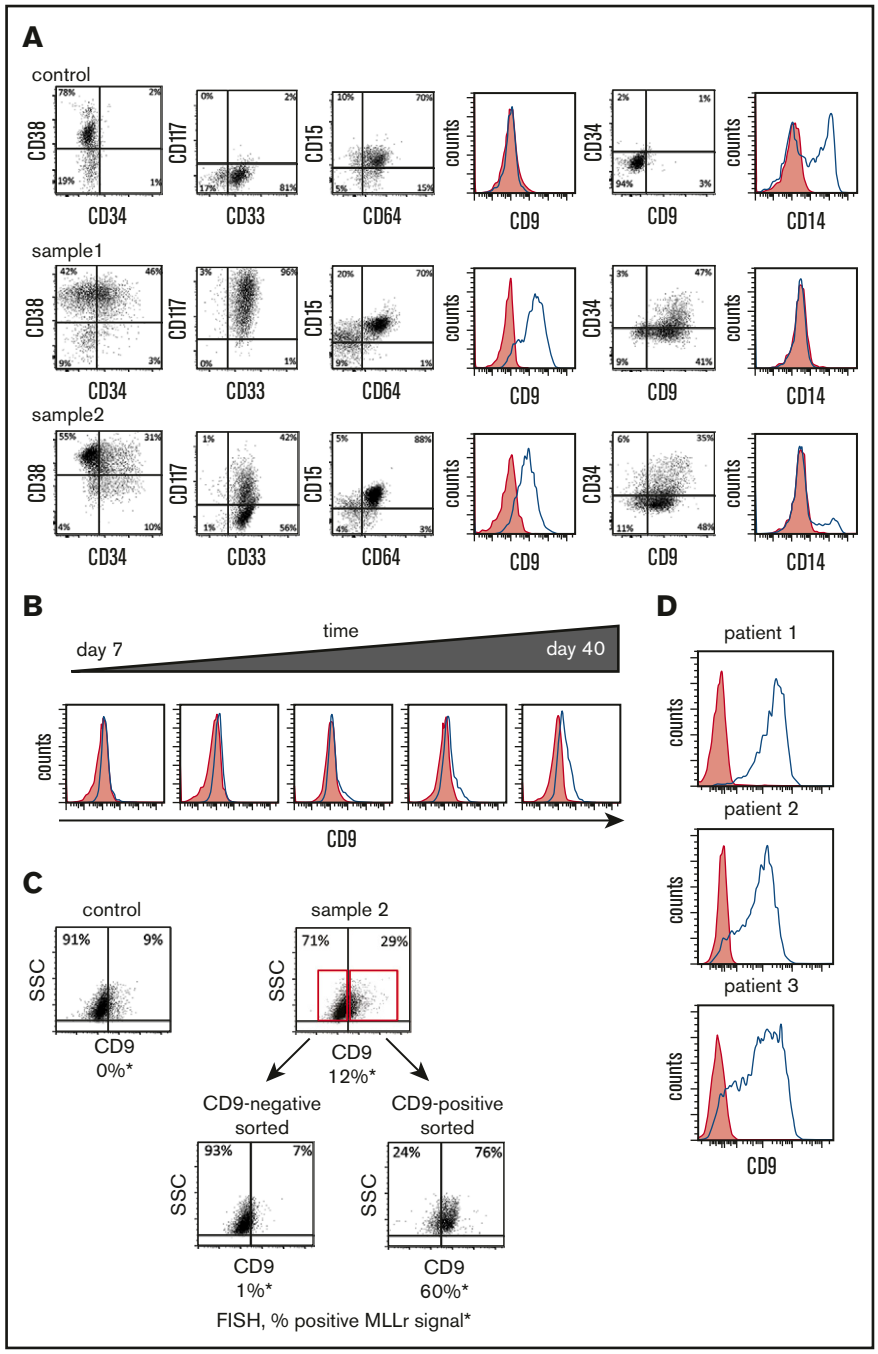

Figure 5. *MLL-AF9* translocated cells preferentially express CD9. (A) Representative flow cytometry analyses are shown for cell-surface protein expression of genome-edited *MLL*r cells compared with control cells ($CD34^+$ cells nucleofected with *GFP* alone) at day 65. (B) Representative flow cytometry plots of CD9 expression over time in culture for genome-edited *MLL*r cells. (C) Representative flow cytometry plots before and after FACS sorting of genome-edited *MLL*r cells based on CD9 expression at day 37 of in vitro culture followed by FISH analysis for *MLL* translocation. (D) Representative flow cytometry plots of CD9 expression on *MLL*r leukemic patient samples. Red shading indicates control (fluorescence minus one); blue line denotes expression of indicated marker. SSC, side scatter.

Human cells were only detected in the peripheral blood at a very late stage of disease progression, and the blood panel was not dramatically changed (data not shown), indicating the disease is primarily localized to the bone marrow and spleen. Leukemic bone marrow cells displayed high expression of CD34, CD117, and CD64 and lack of the differentiation marker CD14 and were CD9 positive at levels similar to injected cells (supplemental Figure 3; compare with Figure 5A). PCR of genomic DNA followed by Sanger sequencing showed monoclonal breakpoint sequences identical to the injected *MLL*r cells (supplemental Figure 4A,C; compare with Figure 1B, arrowheads), and RT-PCR confirmed expression of *MLL-AF9* and *AF9-MLL* fusion transcripts (supplemental Figure 4B). Injection of AML bone marrow cells into secondary recipient mice induced AML with a shorter latency (median 28 weeks, n = 12; Figure 6B; supplemental Figure 5). These results demonstrate that genome editing to create balanced t(9;11) chromosomal translocations transforms primary $CD34^+$ human cord blood cells, leading to acute myelomonocytic leukemia.

The latency observed for AML development in primary transplant recipients, and its acceleration following secondary transplantation, suggested the possibility that collaborating mutations may arise

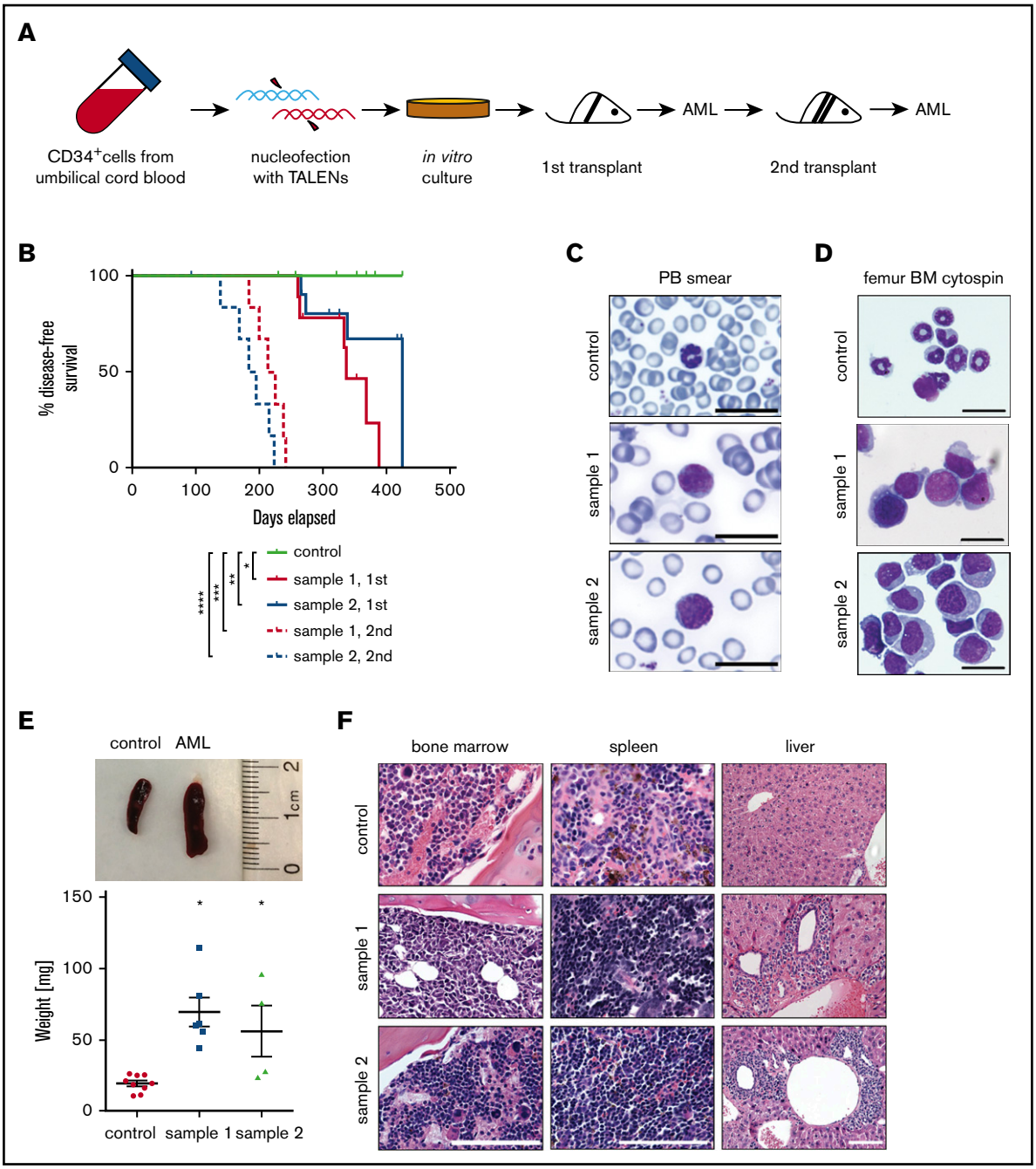

Figure 6. Genome-edited cells with t(9;11) chromosomal translocations induce AML. (A) Experimental scheme for induction of AML by genome-edited cells following transplantation in sublethally irradiated NSG recipient mice after 98 days of in vitro culture. (B) Disease-free survival of transplanted mice; $*P < .009$ (control vs sample 1, 1st), $**P < .07$ (control vs sample 2, 1st), $***P < .0001$ (control vs sample 1, 2nd), and $****P < .0001$ (control vs sample 2, 2nd) by log-rank test. (C-D) May-Grünwald-Giemsa staining shows blast cells in peripheral blood (PB) smear (C) and monomorphic bone marrow (BM) cells (D). Scale bar, 20 μm. (E) Increased spleen size (top) and weight (bottom) of leukemic mice compared with control; $*P < .01$. (F) Hematoxylin and eosin–stained sections of bone marrow, spleen, and liver. Scale bar, 100 μm.

during progression of genome-edited cells in vitro or in vivo. To test this, targeted exome sequencing was performed to assess 53 genes, including *RAS* pathway genes and *FLT3-ITD* (TruSight Myeloid Sequencing Panel, Illumina) that are often mutated in hematological malignancies, including a subset of *MLL*r AML (accession number GSE103811).[23-25] Analysis of mouse leukemia bone marrow cells (n = 2) compared with the original cord blood cells (n = 1), and in vitro–cultured translocated cells at different time points (n = 6), revealed no pathogenic mutations in either leukemic samples or the in vitro culture cells at any time point (data not shown). This prompted a whole-genome approach based on RNA sequencing to identify potential pathogenic expressed single-nucleotide polymorphisms or indels not detected by the targeted exome approach (GSE103811). No recurrent pathogenic secondary

Table 1. Recipient mice transplanted with *MLL-AF9* translocated cells

Injection method (no. of cells)	Injected cells	No. engrafted/no. of mice	AML/no. engrafted
IV (2×10^6)	Control	0/5	0
	Sample 1	4/6	4/4
	Sample 2	4/5	4/4
Intrafemural (1×10^6)	Control	0/4	0
	Sample 1	2/3	2/2
	Sample 2	1/5	0/1

mutations were detected that distinguished the original in vitro genome-edited cells used for transplant (n = 2) from their leukemic counterparts (n = 8 primary leukemia; n = 2 secondary leukemia; supplemental Table 2). Although we cannot exclude that critical additional mutations were not detected in our approach, these results support the possibility that t(9;11) chromosomal translocation is genetically sufficient to induce AML in a human xenograft model.

Unsupervised hierarchical cluster analysis of the RNA-sequencing data demonstrated distinctive gene expression patterns of the various AMLs that clustered separately from the genome-edited cell lines from which they were respectively derived (Figure 7A). Analysis of differentially expressed genes revealed that *MLL*r leukemia signature gene changes, such as upregulation of *HOXA* cluster and downregulation of *HOXB* cluster,[23,26-28] were more prominent in leukemic bone marrow cells than injected cells (supplemental Figure 6A-B). Furthermore, gene set enrichment analysis[29,30] revealed that genes upregulated in human leukemia stem cells (LSCs) were more enriched in the leukemic bone marrow cells compared with the cultured cells, whereas genes downregulated in human LSCs were enriched in the cultured cells used for injection (Figure 7B).[31] These data suggested that LSCs may be more abundant in AML in vivo than in cultured genome-edited cells, consistent with much shorter latencies for disease emergence in secondary transplanted mice (Figure 6B). Thus, although t(9;11) may be sufficient for development of AML from genome-edited primary human cells, environmental or nongenetic factors may also influence disease progression.

Discussion

Using genome editing techniques, we generated t(9;11) chromosomal translocations encoding the *MLL-AF9* and reciprocal *AF9-MLL* fusion products in primary human HSPCs to model the consequences of endogenous oncogene activation in human leukemia. Our studies demonstrate that genome editing is a feasible approach to modify $CD34^+$ huCB cells to induce balanced translocations in a minor fraction of cells, stimulating their long-term clonal outgrowth in supportive cytokine conditions in vitro and promoting leukemia in vivo. Human cells bearing productive translocations driving *MLL-AF9* oncogene expression under control of the endogenous *MLL* promoter, as verified by multiple techniques, induced leukemias in transplanted mice without apparent secondary pathogenic mutations.

Our data are consistent with previous reports showing that genome editing in human cell lines or primary cells can lead to detectable translocations in vitro[11-13] but significantly extend prior studies by demonstrating the leukemic potential of cells with engineered translocations. These advances spurred by the availability of novel genetic tools may provide more representative models to recapitulate the early events in leukemogenesis. However, despite the utility of these techniques, their application remains challenging because of low translocation frequencies, although recent refinements in TALEN[32] and clustered regularly interspaced short palindromic repeats/Cas9[33] methods that are less toxic to transfected primary

Table 2. Pathological features of leukemias arising in mice transplanted with rearranged cells

Mouse number	Injected cells	Latency, d	BM hCD45, %	BM hCD34, %	SP hCD45, %	LV hCD45, %	PB hCD45, %	SP wt, mg	LV wt, mg	Secondary transplant
S1-AML1	S1	259	92.4	53.8	ND	ND	ND	44.0	ND	ND
S1-AML2	S1	335	82.5	30.2	9.5	ND	ND	61.6	865.0	1/2
S1-AML3	S1	386	93.3	51.6	14.27	15.9	ND	55.6	1331.8	ND
S1-AML4	S1	367	98.7	19.3	22.79	17.8	8.88	114.3	1380.9	2/2
S1-AML5	S1	331	94.72	18.1	52.2	7.9	18.6	80.8	1035.2	2/2
S1-AML6	S1	261	84.24	10.9	ND	~1.0	ND	60	3460	ND
S2-AML1	S2	265	94.6	34.7	10.2	ND	ND	96.0	1140	3/3
S2-AML2	S2	272	87.4	43.7	3.0	0.4	ND	23.6	581.6	1/2
S2-AML3	S2	336	66.5	15.6	1.9	0.5	ND	75.8	2367	2/2
S2-AML4	S2	423	54.9	34.9	ND	ND	ND	27.7	ND	ND

h, human; LV, liver; ND, not determined; SP, spleen; wt, weight.

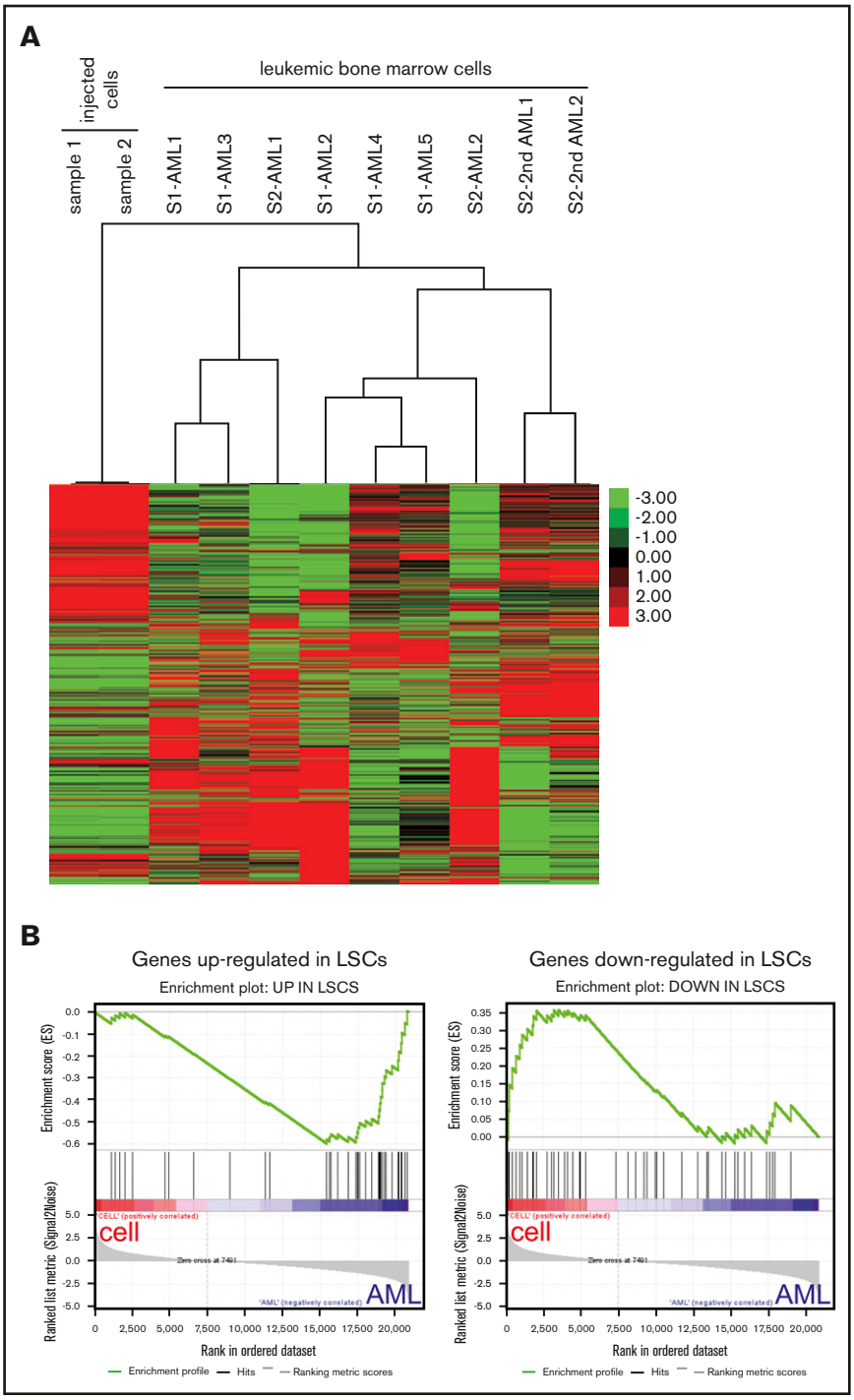

Figure 7. AML signature gene expression changes in the *MLL-AF9* AMLs. (A) Heatmap displays gene expression profiles of *MLL-AF9* rearranged cultured cells and their derived leukemic bone marrow cells. Unbiased hierarchical cluster analysis is shown for 7 primary (AML) and 2 secondary (2nd AML) leukemias compared with 2 cultured cell lines used for injection (S1, sample 1; S2, sample 2). (B) Gene set enrichment analysis plots show that genes upregulated in human LSCs were enriched in the AMLs (left, normalized enrichment score = −1.84, false discovery rate q value = 0) whereas genes downregulated in LSCs were enriched in the injected cells (right, normalized enrichment score = 1.33, false discovery rate q value <0.074).

human cells may allow for increased translocation frequencies. Nevertheless, the genome editing approach employed in our studies addressed these limitations in part by using a cytokine milieu based on the requirements of rearranged cells that lead to their monoclonal outgrowth and replacement of normal hematopoietic elements in vitro comparable to the progressive in vivo development of patient leukemia. The monoclonal outgrowths arose from initial oligoclonal populations of genome-edited cells with diverse *MLL-AF9* translocation breakpoints, suggesting a competitive advantage but nevertheless not associated with detectable secondary mutations in vitro or in vivo. Because the $CD34^+$ HSPCs used for our studies consisted of a mixed hematopoietic cell population, the monoclonal outgrowths may have resulted from translocations occurring in a "primed" stem or precursor population. Further experiments using different subgroups of primary cells are needed to determine which may be most susceptible to initiation by an *MLL* rearrangement.

The frequency of cells with chromosomal translocations generated by genome editing is initially exceedingly low (1 in 300 000 nucleofected cells),[10] and the inability to specifically mark translocated cells complicates efforts for their isolation and study. Expression of CD9 at increased levels by *MLL-AF9* cells may assist in circumventing this limitation. CD9 is a known cell-surface glycoprotein that belongs to the tetraspanin family and is expressed by various hematologic malignancies and solid tumors.[34-38] Recently, Aoki et al described CD9 expression on the surface of *MLL*r ALL cells from patients, whereas normal HSPCs from the same patients did not express CD9.[20] Our studies and analysis of public databases (www.oncomine.org) showed relatively high expression of CD9 in *MLL*r AMLs.[21,22] Thus, although CD9 is not exclusively expressed by *MLL*r leukemia cells, our data suggest that it may serve as a surrogate marker for the detection and possible enrichment of genome-edited HSPCs with t(9;11) from among the much more abundant normal HSPCs in early cultures.

The need for complementing mutations in *MLL* leukemias has been less clear. Genomic analyses of primary patient leukemias show that most *MLL*-associated AMLs do not harbor recurrent secondary mutations, consistent with our results,[26] whereas other studies claim that a majority of *MLL*r AML patients have mutations, especially in Ras pathways.[24,39] In this study, we did not detect recurrent pathogenic mutations, even at hot spots in the *RAS* genes. Although, we cannot exclude possible secondary mutations beyond our detection limit and need more samples for better conclusion, our data suggest that *MLL* rearrangement is sufficient for AML development in cord blood HSPCs. A recent study showed a dynamic relationship between developmental stage and leukemogenic response to *MLL* fusion, where fetal and neonatal hematopoietic progenitors are more sensitive to *MLL-ENL*–driven leukemogenesis than adult cells.[40] It would be interesting to test the effect of *MLL-AF9* translocation in adult hematopoietic progenitors compared with cord blood cells. Nevertheless, our studies clearly demonstrate selection for monoclonal outgrowth of translocated cells in vitro and enrichment of LSCs in vivo. This may reflect the contributions of cell of origin, environmental factors, and/or epigenetic effects as recently discussed for mouse models of *MLL*r leukemia.[41] Our studies provide an experimental platform for further investigation focused on these issues.

Human HSPCs bearing t(9;11) chromosome translocations induced by genome editing developed leukemia, but with relatively long latency. These results differ from those obtained using a genome editing knock-in approach wherein human *MLL-AF9/ENL* leukemias developed within 2 months[9] compared with a median latency of ~11 months in our current study. This may result in part from the longer duration of in vitro culture to obtain sufficient numbers of translocated cells for xenotransplantation. In previous studies, culture of knock-in cells affected leukemia lineage, inducing AML, ALL, and mixed-phenotype acute leukemia when transduced huCB cells were transplanted without antecedent in vitro culture, whereas only AML was observed after 3 weeks of culture prior to transplantation.[9] Restrictive effects of progressive pretransplant culture were also observed following retroviral transduction of *MLL-AF9* or *MLL-ENL* in huCB cells, which initially promoted different human graft phenotypes but eventually extinguished engraftment in immune-deficient mice,[5] whereas induction of leukemia in mice by transformed huCB with the same technique after long-term culture was observed in another report.[42] Our data suggest that despite the competitive growth advantage of genome-edited t(9;11) cells in long-term culture, the frequency of leukemia-initiating cells or their "stemness" properties may be relatively low, possibly due to cytokine addiction of the cells and the lack of those cytokines in NSG mice. Human HSPCs with engineered *MLL* chromosomal translocations appear unable to override the antagonistic effects of progressive in vitro culture on leukemogenesis. This further emphasizes the need for earlier detection and potential enrichment of rare translocated cells for improved *MLL*r leukemia modeling.

In summary, our studies highlight the feasibility of engineering chromosomal translocations at their endogenous loci in primary human cells to induce acute leukemia from initially rare cell populations to model human disease. The genome editing approach demonstrates the ontogeny of *MLL* rearrangements and overcomes the limitations of creating endogenous *MLL* translocations in human HSPCs in vitro, providing the basis for further in vivo studies to prospectively study leukemia etiology and pathogenesis.

Acknowledgments

The authors thank the members of Cleary laboratory for constructive discussions, Carmencita E. Nicolas and Jason H. Kurzer for technical assistance, and Norm Cyr for graphical assistance. The authors also thank Carol D. Jones and Linda Gojenola (Stanford Healthcare) and Jung-Wook Park (University of California, Los Angeles) for help with bioinformatics analysis, Dan Voytas (University of Minnesota) for generously providing the TALEN Golden Gate library, and Daniel E. Vega Salazar (Stanford Hospital) for his efforts and assistance in the collection of huCB.

This work was supported in part by grants from the National Institutes of Health, National Cancer Institute (CA116606) (M.L.C.), Alex's Lemonade Stand Foundation (M.L.C.), Hyundai Hope on Wheels (M.P.), the Dr. Mildred Scheel Stiftung (C.S. and D.S.), the St. Baldrick's Foundation (E.H.B.), the German Research Foundation (J.D.-A.), and the Lucile Packard Foundation for Children's Health (M.L.C.).

Authorship

Contribution: C.S. and J.J. designed and performed the research, analyzed data, and wrote the manuscript; D.S., I.-S.K., E.H.B., J.D.-A, S.H.K.W., and M.I. performed research and analyzed data; J.L.Z. and M.P. provided fruitful discussions; M.L.C. provided overall guidance; and all authors edited the manuscript for content.

Conflict-of-interest disclosure: The authors declare no competing financial interests.

Correspondence: Michael L. Cleary, Department of Pathology, Lokey Stem Cell Research Building, Room G2034, 1291 Welch Rd, Stanford, CA 94305; e-mail: mcleary@stanford.edu.

References

1. Grimwade D, Ivey A, Huntly BJ. Molecular landscape of acute myeloid leukemia in younger adults and its clinical relevance. *Blood*. 2016;127(1):29-41.
2. Muntean AG, Hess JL. The pathogenesis of mixed-lineage leukemia. *Annu Rev Pathol*. 2012;7(1):283-301.
3. Meyer C, Hofmann J, Burmeister T, et al. The MLL recombinome of acute leukemias in 2013. *Leukemia*. 2013;27(11):2165-2176.
4. Wei J, Wunderlich M, Fox C, et al. Microenvironment determines lineage fate in a human model of MLL-AF9 leukemia. *Cancer Cell*. 2008;13(6):483-495.
5. Barabé F, Kennedy JA, Hope KJ, Dick JE. Modeling the initiation and progression of human acute leukemia in mice. *Science*. 2007;316(5824):600-604.
6. Moriya K, Suzuki M, Watanabe Y, et al. Development of a multi-step leukemogenesis model of MLL-rearranged leukemia using humanized mice. *PLoS One*. 2012;7(6):e37892.
7. Chen W, O'Sullivan MG, Hudson W, Kersey J. Modeling human infant MLL leukemia in mice: leukemia from fetal liver differs from that originating in postnatal marrow. *Blood*. 2011;117(12):3474-3475.
8. Chen W, Kumar AR, Hudson WA, et al. Malignant transformation initiated by Mll-AF9: gene dosage and critical target cells. *Cancer Cell*. 2008;13(5):432-440.
9. Buechele C, Breese EH, Schneidawind D, et al. MLL leukemia induction by genome editing of human CD34+ hematopoietic cells. *Blood*. 2015;126(14):1683-1694.
10. Breese EH, Buechele C, Dawson C, Cleary ML, Porteus MH. Use of genome engineering to create patient specific MLL translocations in primary human hematopoietic stem and progenitor cells. *PLoS One*. 2015;10(9):e0136644.
11. Choi PS, Meyerson M. Targeted genomic rearrangements using CRISPR/Cas technology. *Nat Commun*. 2014;5:3728.
12. Piganeau M, Ghezraoui H, De Cian A, et al. Cancer translocations in human cells induced by zinc finger and TALE nucleases. *Genome Res*. 2013;23(7):1182-1193.
13. Torres R, Martin MC, Garcia A, Cigudosa JC, Ramirez JC, Rodriguez-Perales S. Engineering human tumour-associated chromosomal translocations with the RNA-guided CRISPR-Cas9 system. *Nat Commun*. 2014;5:3964.
14. Reimer J, Knöß S, Labuhn M, et al. CRISPR-Cas9-induced t(11;19)/MLL-ENL translocations initiate leukemia in human hematopoietic progenitor cells*in vivo*. *Haematologica*. 2017;102(9):1558-1566.
15. Jansen MW, van der Velden VH, van Dongen JJ. Efficient and easy detection of MLL-AF4, MLL-AF9 and MLL-ENL fusion gene transcripts by multiplex real-time quantitative RT-PCR in TaqMan and LightCycler. *Leukemia*. 2005;19(11):2016-2018.
16. Boitano AE, Wang J, Romeo R, et al. Aryl hydrocarbon receptor antagonists promote the expansion of human hematopoietic stem cells. *Science*. 2010;329(5997):1345-1348.
17. Pabst C, Krosl J, Fares I, et al. Identification of small molecules that support human leukemia stem cell activity ex vivo. *Nat Methods*. 2014;11(4):436-442.
18. Burmeister T, Meyer C, Gröger D, Hofmann J, Marschalek R. Evidence-based RT-PCR methods for the detection of the 8 most common MLL aberrations in acute leukemias. *Leuk Res*. 2015;39(2):242-247.
19. Mitterbauer G, Zimmer C, Fonatsch C, et al. Monitoring of minimal residual leukemia in patients with MLL-AF9 positive acute myeloid leukemia by RT-PCR. *Leukemia*. 1999;13(10):1519-1524.
20. Aoki Y, Watanabe T, Saito Y, et al. Identification of CD34+ and CD34- leukemia-initiating cells in MLL-rearranged human acute lymphoblastic leukemia. *Blood*. 2015;125(6):967-980.
21. Wouters BJ, Löwenberg B, Erpelinck-Verschueren CAJ, van Putten WLJ, Valk PJM, Delwel R. Double CEBPA mutations, but not single CEBPA mutations, define a subgroup of acute myeloid leukemia with a distinctive gene expression profile that is uniquely associated with a favorable outcome. *Blood*. 2009;113(13):3088.
22. Haferlach T, Kohlmann A, Wieczorek L, et al. Clinical utility of microarray-based gene expression profiling in the diagnosis and subclassification of leukemia: report from the International Microarray Innovations in Leukemia Study Group. *J Clin Oncol*. 2010;28(15):2529-2537.
23. Lavallée V-P, Baccelli I, Krosl J, et al. The transcriptomic landscape and directed chemical interrogation of MLL-rearranged acute myeloid leukemias. *Nat Genet*. 2015;47(9):1030-1037.
24. Papaemmanuil E, Gerstung M, Bullinger L, et al. Genomic classification and prognosis in acute myeloid leukemia. *N Engl J Med*. 2016;374(23):2209-2221.
25. Barrett T, Wilhite SE, Ledoux P, et al. NCBI GEO: archive for functional genomics data sets—update. *Nucleic Acids Res*. 2013;41(Database issue):D991-D995.
26. Barabé F, Gil L, Celton M, et al. Modeling human MLL-AF9 translocated acute myeloid leukemia from single donors reveals RET as a potential therapeutic target. *Leukemia*. 2017;31(5):1166-1176.
27. Kharas MG, Lengner CJ, Al-Shahrour F, et al. Musashi-2 regulates normal hematopoiesis and promotes aggressive myeloid leukemia. *Nat Med*. 2010;16(8):903-908.
28. Mullighan CG, Kennedy A, Zhou X, et al. Pediatric acute myeloid leukemia with NPM1 mutations is characterized by a gene expression profile with dysregulated HOX gene expression distinct from MLL-rearranged leukemias. *Leukemia*. 2007;21(9):2000-2009.
29. Mootha VK, Lindgren CM, Eriksson K-F, et al. PGC-1alpha-responsive genes involved in oxidative phosphorylation are coordinately downregulated in human diabetes. *Nat Genet*. 2003;34(3):267-273.

30. Subramanian A, Tamayo P, Mootha VK, et al. Gene set enrichment analysis: a knowledge-based approach for interpreting genome-wide expression profiles. *Proc Natl Acad Sci USA*. 2005;102(43):15545-15550.

31. Ng SWK, Mitchell A, Kennedy JA, et al. A 17-gene stemness score for rapid determination of risk in acute leukaemia. *Nature*. 2016;540(7633):433-437.

32. Knipping F, Osborn MJ, Petri K, et al. Genome-wide specificity of highly efficient TALENs and CRISPR/Cas9 for T cell receptor modification. *Mol Ther Methods Clin Dev*. 2017;4:213-224.

33. Gundry MC, Brunetti L, Lin A, et al. Highly efficient genome editing of murine and human hematopoietic progenitor cells by CRISPR/Cas9. *Cell Rep*. 2016;17(5):1453-1461.

34. Hemler ME. Tetraspanin proteins mediate cellular penetration, invasion, and fusion events and define a novel type of membrane microdomain. *Annu Rev Cell Dev Biol*. 2003;19(1):397-422.

35. Boucheix C, Rubinstein E. Tetraspanins. *Cell Mol Life Sci*. 2001;58(9):1189-1205.

36. Nishida H, Yamazaki H, Yamada T, et al. CD9 correlates with cancer stem cell potentials in human B-acute lymphoblastic leukemia cells. *Biochem Biophys Res Commun*. 2009;382(1):57-62.

37. Murayama Y, Oritani K, Tsutsui S. Novel CD9-targeted therapies in gastric cancer. *World J Gastroenterol*. 2015;21(11):3206-3213.

38. Yamazaki H, Xu CW, Naito M, et al. Regulation of cancer stem cell properties by CD9 in human B-acute lymphoblastic leukemia. *Biochem Biophys Res Commun*. 2011;409(1):14-21.

39. Grossmann V, Schnittger S, Poetzinger F, et al. High incidence of RAS signalling pathway mutations in MLL-rearranged acute myeloid leukemia. *Leukemia*. 2013;27(9):1933-1936.

40. Owuor TO, Porter SN, Cluster A, Ryoo J, Patel R, Magee JA. Fetal and neonatal hematopoietic progenitors are exquisitely sensitive to MLL-ENL-driven leukemia initiation. *Blood*. 2017;130(suppl 1):2473-2473.

41. Milne TA. Mouse models of MLL leukemia: recapitulating the human disease. *Blood*. 2017;129(16):2217-2223.

42. Mulloy JC, Wunderlich M, Zheng Y, Wei J. Transforming human blood stem and progenitor cells: a new way forward in leukemia modeling. *Cell Cycle*. 2008;7(21):3314-3319.